Volume 1 | Number 1 | Jan 2013 | Pages 1–100

Dalton Transactions

An international journal of inorganic chemistry
www.rsc.org/dalton

ROYAL SOCIETY OF CHEMISTRY

ROYAL SOCIETY OF CHEMISTRY

www.rsc.org/dalton

Photosensitized H$_2$ Generation from "One-Pot" and "Two-Pot" Assemblies of a Zinc-Porphyrin/Platinum Nanoparticle/Protein Scaffold

Emily R. Clark and Donald M. Kurtz Jr.*

Department of Chemistry, University of Texas at San Antonio, San Antonio, TX USA

*Address Correspondence to donald.kurtz@utsa.edu.

Abstract

We report photosensitized H_2 generation using a protein scaffold that nucleates formation of platinum nanoparticles (Pt NPs) and contains "built-in" photosensitizers. The photosensitizers, zinc-protoporphyrin IX or zinc-mesoporphyrin IX (ZnP) were incorporated in place of the naturally occurring heme in the 24-subunit iron storage protein bacterioferritin (Bfr) when the ZnPs were added to the *E. coli* expression medium. We engineered a stable dimeric Bfr variant with two protein subunits sandwiching a ZnP. Ten glycines were also substituted in place of residues surrounding the vinyl side of the porphyrin in order increase access of solvent and/or redox agents. An optimized "one-pot" reaction of this glycine-substituted ZnMP-Bfr dimer with a Pt(IV) salt and borohydride resulted in a ~50:50 mixture of protein in the form of Pt-free glycine-substituted ZnP-Bfr dimers and re-assembled 24-mers surrounding Pt NPs formed in situ. H_2 production occurred upon visible light irradiation of this "one-pot" product when combined with triethanolamine as sacrificial electron donor and methyl viologen as electron relay. An analogous "two-pot" system containing mixtures of separately prepared Pt-free glycine-substituted ZnP-Bfr dimer and porphyrin-free Pt NP@Bfr 24-mer also showed robust photosensitized H_2 generation. The glycine-substituted-ZnP-Bfr dimer thus served as photosensitizer for catalytic reduction of methyl viologen by triethanolamine, and the reduced methyl viologen was able to transfer electrons across the Bfr 24-mer protein shell to generate H_2 at the enclosed Pt NP in a "dark" reaction. Our results demonstrate that Bfr is a readily manipulatable and versatile scaffold for photosensitized redox chemistry.

Introduction

Efficient solar-driven splitting of water: $2H_2O \rightarrow 2H_2 + O_2$, using inexpensive, "green" and "earth abundant" materials is a holy grail.[1] One approach to this goal has been to assemble systems that separately photo-drive each of the two half reactions, i.e., either reduction or oxidation of water. Numerous synthetic, biomimetic, and synthetic/biological hybrid approaches to photosensitized reduction of water to H_2 have been described.[2-6] Several such examples using porphyrins as photosensitizers are known.[7, 8] One of the earliest such aqueous systems, diagrammed generically in Scheme 1, used a zinc(II)-porphyrin (ZnP) as photosensitizer, a sacrificial electron donor (SED, typically a tertiary amine), and methyl viologen (MV) as an electron relay to colloidal platinum (Pt), where H_2 production occurred.[9-11] MV^{2+} is a well established oxidative quencher of photo-generated Zn(II)-porphyrin triplet states ($^3ZnP^*$),[12, 13] and MV^+ has been shown to supply reducing equivalents for generation of H_2 on colloidal Pt in a separate "dark" reaction.[14] The earliest examples used synthetic ZnPs with high positive charge in order to improve water solubility and inhibit porphyrin aggregation. ZnPs derived from naturally occurring porphyrins, such as protoporphyrin IX, tend to aggregate in aqueous solution, which quenches the $^3ZnP^*$, thereby attenuating its redox efficiency. An approach to preventing this aggregation has been to substitute Zn(II)-protoporphyrin IX and related ZnPs into heme binding sites in proteins, thereby spatially isolating individual ZnP molecules.[12, 13, 15]

Scheme 1
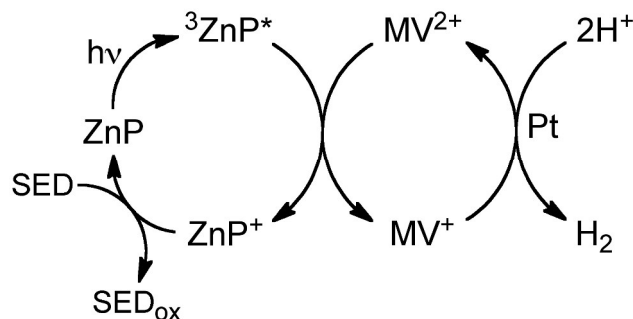
Platinum NPs (Pt NPs), which are frequently used as a hydrogen-evolving catalyst, have been successfully incorporated into cage-like proteins[16-18] and in a few cases used with exogenous metal-based photosensitizers to generate H_2.[19-21] Bacterioferritin (Bfr) is a bacterial iron storage protein analogous to mammalian ferritin.[22] We used the Bfr from *Escherichia* (*E.*) *coli*, which is the most extensively characterized and is representative of the Bfr family. Structural and functional features of *E. coli* Bfr are shown in Figure 1. The protein is composed of 24 identical 18.5-kD subunits arranged as 12 head-to-tail homodimers forming an approximately spherical cage (Figure 1A) with an ~8-nm interior cavity (Figure 1B). This cavity can store up to 3,000 iron atoms as a ferric oxyhydroxide.[23, 24] Unlike all other known ferritins, the Bfr 24-mer can stably bind up to 12 heme groups sandwiched between head-to-tail subunit pairs, as shown in Figure 1C. The hemes are separated from each other by ~4 nm, and the heme irons are axially ligated by two methionine sulfurs, one from each subunit (Figure 1D), thereby bridging the 12 dimer interfaces.[25] The propionate side of the heme (Scheme 2) projects into the interior cavity. Direct solvent access to the opposite (vinyl) side of the heme is obstructed by surrounding surface loops (Figure 1C). However, crystal structures of several Bfrs (including multiple crystal structures of *E. coli* Bfr)[26-28] show that the heme vinyl side projects into a buried pocket, which is occupied by a hydrogen-bonded network of water molecules (Figure S1). The hemes may be involved in the redox chemistry of iron uptake or release, although this issue remains to be clarified.[22]
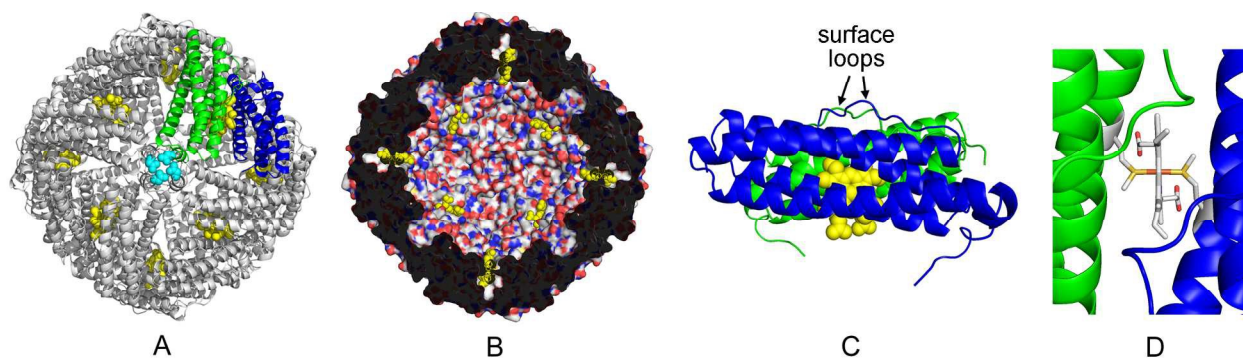
Figure 1. Structural features of the *Escherichia* (*E.*) *coli* Bfr 24-mer (wtBfr) **(A)** protein backbone viewed along a four-fold rotational axis with hemes highlighted in yellow, N148 residues around one of the four-fold axes highlighted in cyan, and two head-to-tail dimer subunits highlighted as a blue/green pair. **(B)** Slice through a surface rendering (oriented as in **(A)**) showing the ~8-nm interior cavity and hemes (yellow) embedded in the protein shell. **(C)** View of a head-to-tail homodimer with embedded heme (yellow spheres) and surface loop regions above the vinyl side indicated. **(D)** View of a head-to-tail homodimer along the heme plane (stick rendering) showing axial methionine ligands to iron. Drawings were generated in PyMOL (Schrödinger LLC) using coordinates from Protein Data Bank entry, 1bfr.[29]

Scheme 2

heme, X = vinyl

ZnPP, X = vinyl
ZnMP, X = ethyl
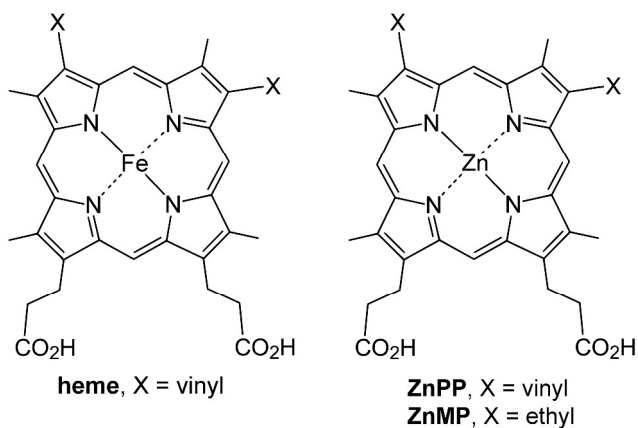
We reasoned that replacing the heme with a structurally analogous ZnPs (Scheme 2) could create a protein with "built-in" photosensitizers capable of housing a Pt NP. Substitution of the heme in Bfr with a Zn(II)-chlorin photosensitizer has in fact been previously reported.[30] Here we describe "one-pot" and "two-pot" assemblies of a Pt NP/ZnP system using Bfr containing either Zn(II)-protoporphryin IX (ZnPP) or Zn(II)-mesoporphyrin IX (ZnMP) and their photosensitized generation of H_2.

Materials and Methods

Materials

All aqueous solutions were prepared in water that had been passed through a Milli-Q® ultrapurification system (Merck Millipore, Inc.) to achieve a resistivity of 18 MΩ. All manipulations involving ZnP and ZnP-Bfrs were carried out in reduced room light. Porphyrins were purchased from Frontier Scientific.

Syntheses of ZnP

ZnPs were prepared by metallation of MP or PP with zinc acetate dihydrate adapted from a published method.[31] 70 mg of the porphyrin was dissolved in 15 mL HPLC-grade dimethylsulfoxide (DMSO). Solid zinc acetate dihydrate equimolar to the porphyrin was added, and the solution was refluxed for 30 min. Zinc incorporation into the porphyrin was monitored by the Soret and Q-band shifts in the UV-vis absorption spectrum. This in situ DMSO solution of ZnP was added directly to 1 L *E. coli* cell cultures used for Bfr overexpression.

Bfr overexpression and purification

The expression plasmid encoding *E. coli* Bfr, hereafter referred to as wtBfr (wild type Bfr), has been described previously.[32] The plasmid encoding a Bfr N148D variant, hereafter referred to as Bfr dimer, was prepared using the QuikChange® method (Agilent Technologies) with the wt Bfr expression plasmid as template. The plasmid encoding a six-residue Bfr variant, N23G/L71G/Q72G/D73G/L74G/N148D, hereafter referred to as 5gly-Bfr dimer, was synthesized by GenScript (Piscataway, NJ) with codons optimized for expression in *E. coli* and inserted into the overexpression plasmid, pT7-7 (the same parent plasmid used for expression of wtBfr).[33] *E. coli* BL21(DE3) transformed with the expression plasmids. These transformed strains were grown in Luria-Bertani broth containing 100 mg/L ampicillin at 37°C. Overexpression of the ZnP-containing proteins (ZnP-wtBfr, ZnP-Bfr dimer, and ZnP-5gly Bfr dimer) was induced in shaking 1-L cultures at 37 °C by the addition of 100 mg isopropyl-beta-D-thiogalactoside (IPTG) when OD_{600} of the cultures reached 0.5–0.7, followed immediately by addition of 70 mg ZnP in 15 mL DMSO. After four hours incubation with shaking at 37 °C the cells were harvested from the cultures by centrifugation. Porphyrin-free wtBfr was overexpressed from cultures grown in M9 minimal medium containing 100 mg/L ampicillin. 1-L cultures were incubated with shaking at 37°C until OD_{600} reached ~0.4, at which point, the temperature of the cultures was lowered to 25°C. When OD_{600} reached ~0.6, 100 mg IPTG was added. After overnight shaking of the cultures at 25°C, the cells were harvested by centrifugation.

Porphyrin-free wtBfr, ZnP-wtBfr, ZnP-Bfr dimer and ZnP-5gly-Bfr dimer were isolated and purified as follows. The cell pellets from six 1 L cultures were frozen at -80 °C overnight,

then thawed and suspended in 50 mM 3-(*N*-morpholino)propanesulfonic acid (MOPS) pH 7.4, 5 mM $MgSO_4$, RNAse and DNAse. The re-suspended cells were lysed by sonication and cell debris was removed by centrifugation (20,000 x g, 1 h). The supernatant was applied to a 10 mL anion-exchange column (HiTrap Q X L, GE Healthcare), and the Bfr was eluted with 50 mM MOPS, 1 M NaCl pH 7.4. The eluted protein was then applied to a 100 mL aluminum foil-covered column containing Sephacryl-200 resin (GE Healthcare) and eluted with 50 mM MOPS, 0.5 M NaCl, pH 7.4. For the ZnP-containing Bfrs UV-visible absorption spectra of eluted fractions were obtained using a NanoDrop ND-1000 spectrophotometer, and fractions with an A_{433nm}/A_{280nm} ratio of ~ 2 were combined, concentrated, and washed with 50 mM MOPS pH 7.4. The ZnP-Bfrs were stored at -80°C in aluminum foil-covered Eppendorf tubes.

Loading Bfrs with Pt NPs

All reactions were carried out at room temperature in solutions containing 50 mM MOPS pH 7.4 and 0.5 μM porphyrin-free wtBfr 24-mer, 0.5 μM ZnP-wtBfr 24-mer, 6 μM ZnP-Bfr dimer or 6 μM ZnP-5gly-Bfr dimer. Typical reaction volume was 3.5 mL. K_2PtCl_4 was added from a concentrated stock solution to achieve Pt concentrations of either 0.4 mM or 0.8 mM. After two hours incubation, sodium borohydride was added from a freshly prepared aqueous stock solution to achieve concentrations of either 0.2 or 0.4 mM (0.5 mol borohydride per K_2PtCl_4). The solutions were stirred for 60 min. Insoluble Pt in the form of a black precipitate was removed by centrifugation at 10,000 x g for 5 min. Buffer was exchanged into 50 mM 2-(*N*-morpholino)ethanesulfonic acid (MES) 0.5 M NaCl, pH 6, and excess reagents were removed by either passage over desalting columns (Econo-Pac 10DG column, Bio-Rad) or dialysis (Slide-a-Lyzer® Dialysis Cassette, Thermo Scientific).

Quantifications and Characterizations

Protein was quantified by a 660 nm Protein Assay (Thermo Scientific Pierce). ZnP concentrations were determined by UV-visible absorption using molar extinction coefficients, $\varepsilon_{433} = 114$ mM^{-1}cm^{-1} for ZnPP-Bfr dimer, $\varepsilon_{427} = 102$ mM^{-1}cm^{-1} for ZnPP-5gly-Bfr dimer, $\varepsilon_{424} = 111$ mM^{-1}cm^{-1} for ZnMP-Bfr dimer, and $\varepsilon_{415} = 96$ mM^{-1}cm^{-1} for ZnMP-5gly-Bfr dimer. These extinction coefficients were determined from modified pyridine hemochromogens,[34] which were prepared by diluting the ZnPP-Bfrs or ZnMP-Bfrs with 40% (v/v) pyridine in 200 mM NaOH. The absorption standard was a pyridine/NaOH solution of a known concentration of ZnP prepared from a weighed quantity of commercial ZnP (Frontier Scientific, ≥95% purity by HPLC). Non-heme iron content was measured by either ferrozine assay[35] or inductively coupled plasma-optical emission spectrometry (ICP-OES). Pt content was determined by ICP-OES. Fluorescence emission spectra of 60 μM 5gly-ZnPP-Bfr dimer and 60 μM ZnPP-Bfr dimer in 50 mM MES 0.5 M NaCl, pH 6 at 502 nm were obtained using a SpectraNet fluorimeter. ZnMP concentrations in the "one-pot" samples were determined by UV-vis absorption spectrophotometry of the Soret band immediately after Pt loading and also after separating the Pt-loaded fractions into dimer and 24-mer using size-exclusion chromatography (SEC). (SEC dimer fractions did not contain Pt NPs, allowing for better visualization of the ZnP Soret absorption without interference from Pt NP light scattering). SEC was performed on a Superose 6 10/300 GL column (GE) equilibrated with 50 mM MOPS 150 mM NaCl, pH 7.4. Protein molecular weights were determined using a standard curve of carbonic anhydrase, ovalbumin, conalbumin, apoferritin, and thyroglobulin (GE). 100 - 200 μL of ~ 0.4 mg/mL protein was loaded onto the column and eluted at 0.4 mL/min with the same buffer while monitoring absorbance at 280 nm. TEM was preformed on a JEOL-2010F microscope operated at 200kV.

Samples were prepared on ultrathin holey carbon-coated copper grids (Ted Pella) and negatively stained with 2% uranyl acetate.

Photosensitized reduction of MV^{2+}

Solutions contained 2 mM MV^{2+}, 0.1 mM TEOA, and 10 μM ZnP-Bfr in 2-(N-morpholino)ethanesulfonic acid (MES) pH 6. 2 mL of the solution was placed in a quartz cuvette sealed with a screw cap and rubber septum and made anaerobic by repeated evacuation and filling of the headspace with N_2 gas via syringe needle connected to a vacuum line. Irradiations were carried out at room temperature using a 300-W halogen lamp focused through a slide projector lens with the sample vial placed 5-10 cm from the lens. UV-visible absorbance spectra were recorded every 15 minutes on an Ocean Optics USB 2000 spectrophotometer.

Photosensitized generation of H_2

All irradiated solutions contained the indicated concentrations of Pt NP and ZnP-5gly-Bfr, as well as 2 mM MV^{2+}, 0.5M NaCl, and 0.1 M TEOA in 50 mM 2-(N-morpholino)ethanesulfonic acid (MES) pH 6. 3.5 mL of the solution was placed in a 6.5 mL cylindrical glass screw cap vial (Chemglass), and the vials were left uncapped overnight in an N_2-filled glove box (Vacuum atmospheres Co.) at 4 °C in order remove O_2. The vials were then sealed with a rubber septum Mininert® cap and removed from the glove box. Continuous irradiations were carried out at room temperature on stirred solutions using a 300-W halogen lamp focused through a slide projector lens with the sample vial placed 5-10 cm from the lens. Light irradiance at the sample was measured using a Konica Minolta CL-500A Illuminance spectrophotometer. H_2 production was monitored by periodic withdrawal of 100 – 250 uL of

headspace gas into a gastight syringe and injection into a Varian CP-3800 gas chromatograph equipped with a Carboxen™ 1010 PLOT (Supelco) column and thermal conductivity detector. The column was calibrated for amount of H_2 using a standard curve prepared from a series of solutions with varying known amounts of H_2 gas (Sigma-Aldrich) injected into buffer in the same type of reaction vials used for photosensitized H_2 generation.

Results and Discussion

Protein isolation and characterization

In addition to the *E. coli* wtBfr we engineered two variants. Asparagine148 surrounds the six four-fold rotationally symmetric channels of the 24-mer (Figure 1A), and we found that replacing N148 with the negatively charged aspartate side chain caused dissociation of the 24-mer into stable homodimers (verified by SEC, see below). We refer to this N148D variant as Bfr dimer. We created an additional variant based on the observation that the vinyl side of the heme is buried under loop regions (Figure 1B, Figure 1C). We sought to increase solvent and/or reagent access to the vinyl side by substituting four residues in these loops with glycines (L71G/Q72G/D73G/L74G). We also made a fifth substitution (N23G) of a more buried residue lying near the vinyl edge of the heme (Figure S1). Two sets of these five residues are symmetrically disposed around each heme. For simplicity we refer to this engineered variant containing both N148D and the five residues substituted with glycines as 5gly-Bfr dimer. We used the SWISS-MODEL web server (http://swissmodel.expasy.org/) to obtain a structural model of the 5gly-Bfr dimer using its amino acid sequence and the crystal structure of an alternative *E. coli* heme-containing Bfr dimer variant (PDB ID 3e2c) as template.[26] A comparison of solvent contact surfaces in the 5gly-Bfr dimer structural model with that of the

3e2c crystal structure (Figure 2) indicates that substitution with the ten total glycine residues on the Bfr dimer opens a channel to the buried, water-filled pocket (Figure S1) leading from the vinyl side of the porphyrin to the protein surface. The putative enlargement of the pocket and channel together with greater loop flexibility expected from the ten glycine substitutions could lead to increased solvent and/or reagent access to the vinyl side of the ZnP.
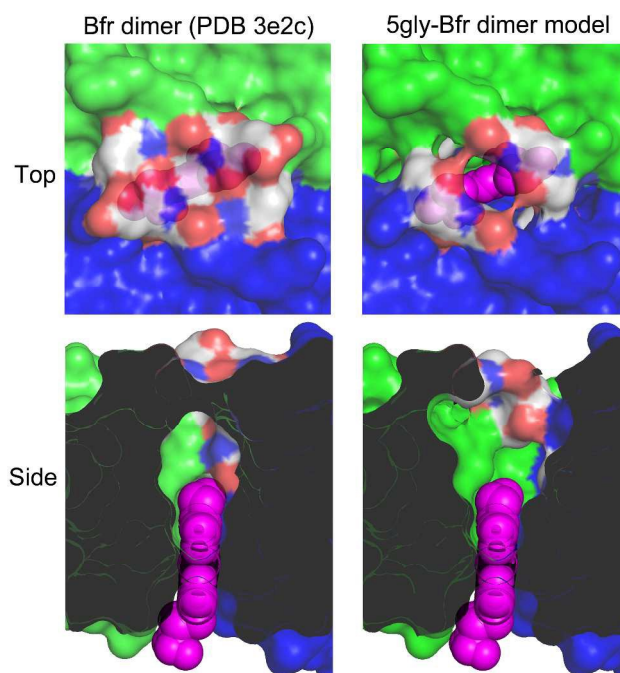
Figure 2. Solvent/protein molecular contact ("Connolly") surfaces surrounding the heme in the crystal structure of a Bfr dimer (PDB entry 3e2c) (left panels) and in a structural model of the 5gly-Bfr dimer (right panels). Protein subunits are colored blue or green. Residues 23, 71-74 side chains are highlighted in CPK colors. Heme atoms are represented as magenta spheres. "Top" indicates views from the surface above the protein loops (indicated in Figure 1C), which surround the vinyl side of the heme. "Side" indicates views approximately perpendicular to the "Top" views and parallel to the heme plane with cross-sections through the subunits. Surface renderings were generated in PyMOL (Schrödinger LLC). Hydrogen atoms were not included.

The wtBfr as well as the Bfr dimer and 5gly-Bfr dimer variants were all isolated with essentially quantitative incorporation of ZnPP or ZnMP (~1 ZnP per dimer) when ZnP was added to the *E. coli* culture medium at the time of induction of protein expression. The ZnPs remained irreversibly bound to the wtBfr, Bfr dimer, and 5gly-Bfr dimer under the conditions used for the studies described here. We refer to these proteins as ZnP-wtBfr, ZnP-Bfr dimer and ZnP-5gly-Bfr dimer. The UV-vis absorption spectra (Figure 3) of ZnP-wtBfr and ZnP-Bfr dimer are essentially superimposable. The spectra of the 5gly-ZnP-Bfr dimers showed small blue shifts in both the Soret and Q bands compared to the corresponding spectra ZnP-Bfr dimers, indicating some perturbation of the porphyrin environment induced by the glycine substitutions. Minor perturbations were also evident in the fluorescence emission spectra (Figure S2).

Under the same expression conditions, a Bfr variant in which the heme-ligating methionine residue was substituted with leucine (M52L) failed to bind any ZnP (Pacheco, E., Kurtz, D. M. Jr., unpublished). The M52L variant was previously shown not to bind heme even though it formed a stable 24-mer.[25] This observation and the narrow spectral bandwidths shown in Figure 2 are consistent with ZnP insertion specifically into the heme binding site of Bfr. The nature of the axial ligation in these ZnP-Bfrs is unclear. Established examples of six-coordinate Zn(II)-porphyrins are extremely rare.[36] While the UV-vis and fluorescence spectra of the ZnP-Bfrs reported here generally resemble those of five-coordinate ZnPs in other proteins,[12, 31, 37-39] we have found no reports of a five-coordinate, thioether-ligated Zn(II)-porphyrin.
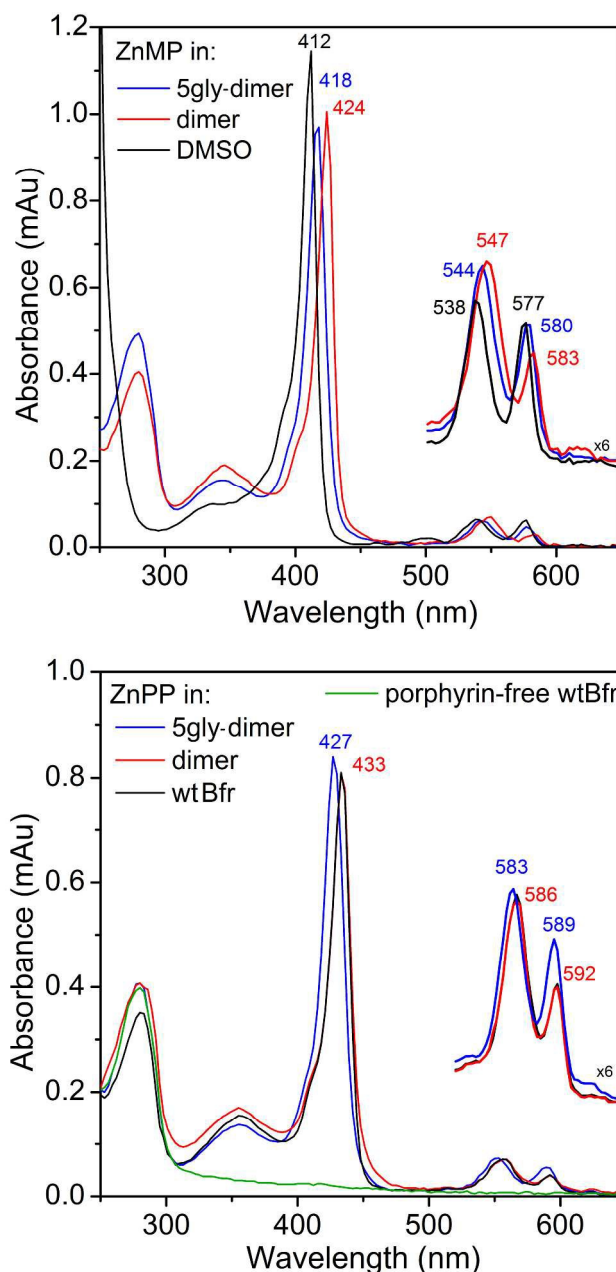
Figure 3. UV-visible absorption spectra of Bfr and dimer variants used in this study. Spectra were recorded of protein solutions in 50 mM MES + 0.5 M NaCl, pH 6 at 50 μM porphyrin.

When wtBfr was expressed from cultures grown in minimal media containing no added heme or porphyrin, the isolated Bfr showed little or no porphyrin absorption (Figure 3B), and we refer to this protein as porphyrin-free wtBfr. Non-heme iron in the as-isolated variant Bfrs was

14

usually undetectable, and that in the porphyrin-free wtBfr never exceeded 3 irons per subunit. Based on ICP-OES, any residual iron was apparently removed during the platinum salt/borohydride treatment described below. A 5gly-Bfr variant containing the native N148 formed a 24-mer, but for unknown reasons did not stably bind ZnPP or ZnMP.

The photochemical behavior of the ZnPP-containing Bfrs paralleled those of the ZnMP-Bfrs. For brevity the results reported below are confined to the ZnMP-containing Bfrs. Parallel results for the ZnPP-containing Bfrs are contained in the Supplementary Information.

Photosensitization by ZnMP-Bfrs

The UV-vis absorption spectral time courses in Figure 4 show that the various ZnMP-containing Bfrs can photosensitize reduction of MV^{2+} to $MV^{•+}$ by the SED, triethanolamine (TEOA).[12] Both the rate and extent of $MV^{•+}$ formation during 4 hours of continuous white light irradiation was significantly higher with ZnMP-Bfr dimer compared to ZnMP-wtBfr and higher still using the ZnMP-5gly-Bfr dimer. The higher yield of $MV^{•+}$ using the ZnMP-Bfr dimer in place of ZnMP-wtBfr (24-mer) could be explained by increased access of MV^{2+} and/or TEOA to the propionate side of the ZnMP, which is oriented towards the inner cavity of the 24-mer (Figure 1C,D). The additional increase in efficiency of photosensitized MV^{2+} reduction upon substitution with the ten glycine residues per ZnP is consistent with the increased exposure of the vinyl side of the ZnP in the 5gly-Bfr dimer structural model (Figure 2). Parallel behavior for the ZnPP-containing proteins is shown in Figure S3.
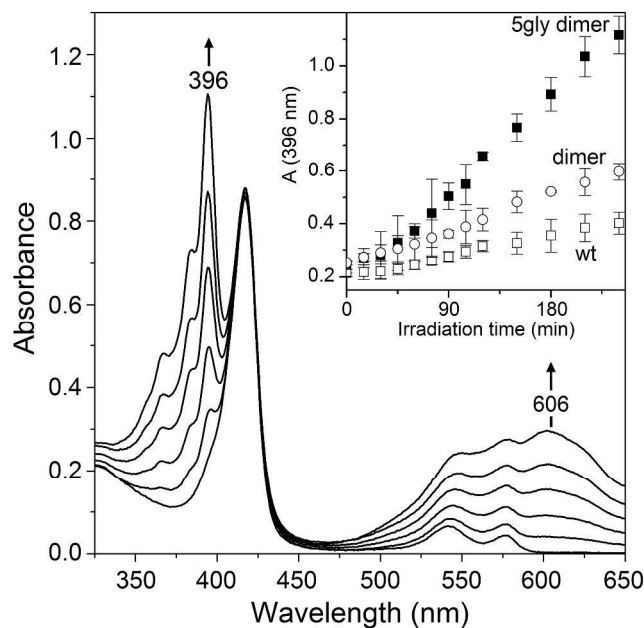
Figure 4. UV-vis absorption spectral time course of MV^{2+} reduction to $MV^{\bullet+}$ induced by irradiation with white light from a 300 W halogen lamp (3.8 mW/cm^2) of an anaerobic solution containing 10 µM ZnMP-5gly Bfr dimer, 2 mM MV, and 0.1 M TEOA in 50 mM MES, 0.5 M NaCl pH 6. Positions of $MV^{\bullet+}$ absorption maxima at 396 nm and 606 nm are indicated. Arrows indicate absorbance increased with time. The absorption features at ~424, 540 and 580 nm are due to the ZnMP. Inset: $A_{396\ nm}$ time courses for MV^{2+} reduction using 10µM ZnMP-5gly Bfr-dimer (closed squares), ZnMP-Bfr dimer (open circles), or ZnPP-wtBfr (open squares). Data points are the average of from at least three experiments with error bars representing standard deviations.

Pt NP incorporation

Pt NPs were incorporated into the various Bfrs by reduction in an optimized "one-pot" reaction by addition of K_2PtCl_4 at a mol ratio of 66 Pt/Bfr dimer followed by addition of $NaBH_4$. The ZnMP Soret in the 5gly-Bfr dimer band remained intact during Pt reduction and was

16

superimposed on background light scattering by the Pt NPs (Figure 5A). These solutions

remained transparent with no precipitate, whereas control reactions omitting protein resulted in a

black precipitate. After workup of the 66 Pt/ZnMP-5gly-Bfr dimer/borohydride reaction

mixtures as described in Materials and Methods, mol ratios of 43 Pt/protein dimer (~520

Pt/effective 24-mer) were obtained. SEC (Figure 5B) and transmission electron microscopy

(TEM) (Figure S4A) showed that this "one-pot" Pt/ZnMP-5gly-Bfr dimer preparation contained

40 – 50% of the protein as dimer and the remainder as 24-mer (or 24-mer-like structures)

surrounding Pt NPs. Only the SEC dimer fractions showed porphyrin absorption features. The

protein-encapsulated Pt NPs had a diameter range of 1.5 – 6 nm with a mean of 2.7 nm (Figure

S5A). The relatively broad SEC bands of the 24-mer component can be ascribed to the

distributions of NP sizes.
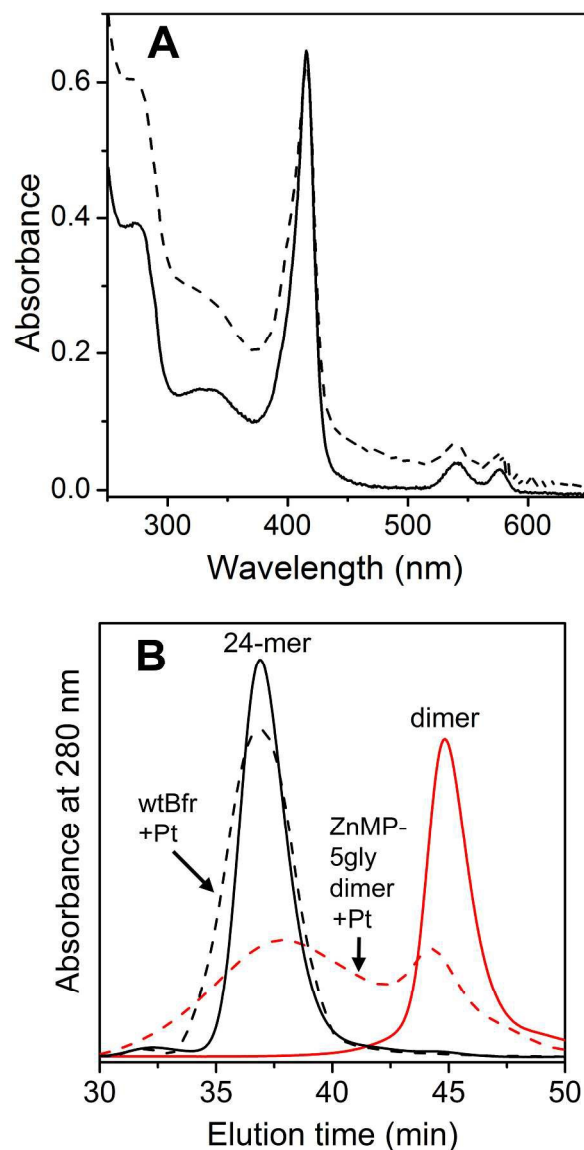
Figure 5. (A) UV-vis absorption spectra of 6 μM ZnMP-5gly-Bfr dimer + 0.4 mM K$_2$PtCl$_4$ (66

Pt per Bfr dimer) before (solid) and after (dashed) addition of 0.2 mM NaBH$_4$ and workup (see

Materials & Methods). All reactions were carried out at room temperature in 50 mM MOPS, pH

7.4. **(B)** Size exclusion chromatograms (SECs) of: porphyrin-free wtBfr (black, solid), ZnMP-

5gly-Bfr dimer (red, solid), post-workup sample from reaction of porphyrin-free wtBfr with

K$_2$PtCl$_4$/NaBH$_4$ at 1600 Pt/24-mer (black, dashed), or post-workup sample from reaction of

ZnMP-5gly-Bfr dimer with K$_2$PtCl$_4$/NaBH$_4$ at 66 Pt per/Bfr dimer (red, dashed).

The ZnMP-5gly-Bfr dimer is, thus apparently capable of assembling into a 24-mer (or 24-mer-like structure) when surrounding Pt NPs, which we envision occurring as diagrammed in Scheme 3.

Scheme 3
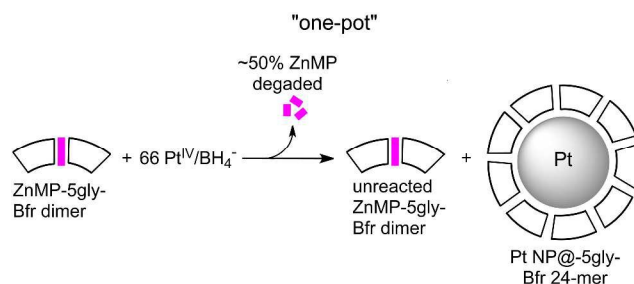
Consistent with the interpretation in Scheme 3, analogous reactions in which the Pt salt concentration was doubled to 133 Pt per ZnMP-5gly-Bfr dimer resulted after workup in SEC chromatograms and TEM and showing 80 – 90% of the protein in the form of 24-mers surrounding 1.5 – 6 nm Pt NPs (Figure S6). However, this higher Pt loading was accompanied by a substantial loss of the porphyrin Soret absorption (presumably due to degradation by the higher borohydride/protein ratio) and higher background scattering, which rendered these preparations unsuitable for photosensitized H_2 generation (see below). Similar oligomeric proportions and porphyrin contents were obtained from analogous reactions using ZnMP-Bfr dimer in place of ZnMP-5gly-Bfr dimer at 66 or 133 Pt/ZnMP-Bfr dimer.

Analogous reaction of K_2PtCl_4/$NaBH_4$ with porphyrin-free wtBfr using 1600 mol Pt/mol 24-mer resulted in > 90% of the protein in the form of 24-mers surrounding Pt NPs with diameters of 2.5 - 5 nm (Figure 5B, Figure S4B and Figure S5B). Pt salt/borohydride reactions with the ZnMP-wtBfr resulted in significant porphyrin degradation. Attempts to incorporate ZnPs into the porphyrin-free wtBfr after Pt NP incorporation were unsuccessful.

Photosensitized H$_2$ generation

As shown in the "One-pot" panel of Figure 6, in the presence of TEOA and MV, we observed photosensitized production of H$_2$ for "one-pot" preparations containing the ZnMP-5gly-Bfr dimer in which SEC and TEM showed an ~50:50 mixture of protein as Pt-free Bfr dimer and Pt NP@Bfr 24-mer. White light irradiation of "one-pot" post workup samples containing 5.3 ± 0.2 μM 5gly-ZnMP-Bfr dimer (estimated by protein assay and Soret absorption of the dimer fraction collected from SEC) and 123 ± 5 μM Pt generated 0.89 ± 0.01 micromol H$_2$ after 4 hours. No precipitation was observed before, during, or after irradiation for up to 5 hours. Control experiments in which any one of MV^{2+}, TEOA or Pt-treated protein was omitted resulted in no detectable photogeneration of H$_2$. Similarly, no "dark" generation of H$_2$ was observed in the complete mixture. After 4 hours of irradiation, the ZnMP Soret band was no longer detectable in the UV-vis absorption spectrum, which suggests that porphyrin degradation is responsible for the leveling off of H$_2$ generation after 4 hours. The 0.9 micromol H$_2$ represents a turnover of ~60 H$_2$/ZnMP (probably a lower limit given the porphyrin photodegradation). An analogous "one-pot" preparation of ZnMP-Bfr dimer generated no detectable H$_2$ during four hours of continuous irradiation (Figure 6, "One-pot" panel).
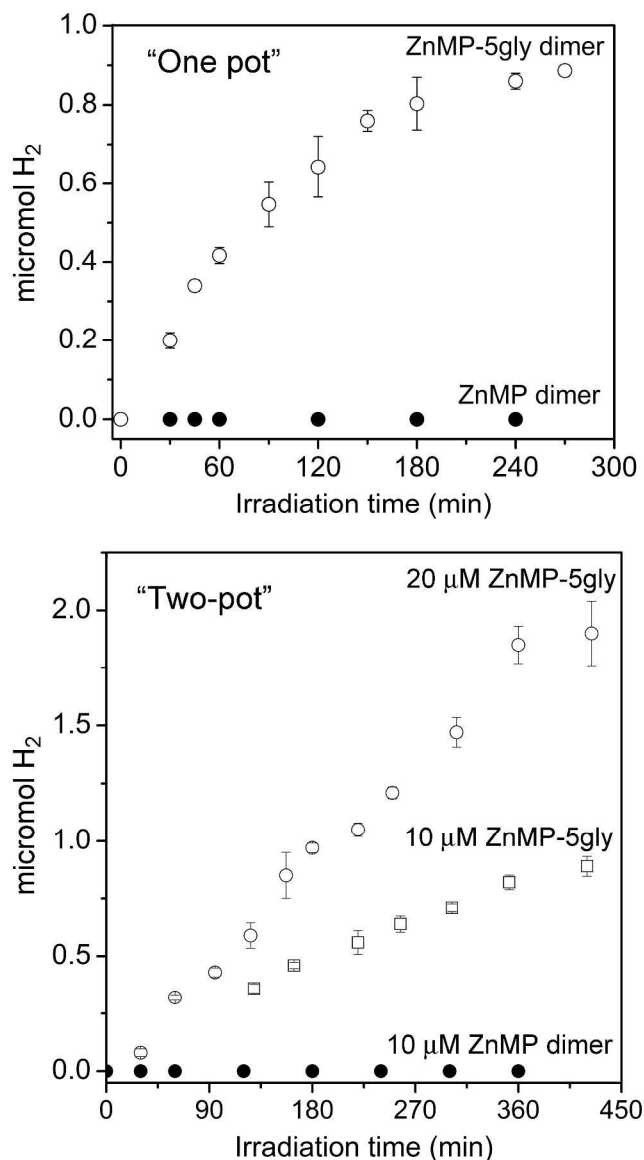
Figure 6. Time dependence of photosensitized H_2 production using either "one-pot" preparations or "two-pot" mixtures. (Top panel) "One-pot" samples were from 66Pt/Bfr dimer preparations and contained ~120 μM Pt and ~ 5 μM of either ZnMP-Bfr dimer (closed circles) or ZnMP-5gly-Bfr dimer (open circles). (Bottom panel) "Two-pot" mixtures all contained porphyrin-free Pt NP@wtBfr at 20 μM Pt and either ZnMP-Bfr dimer (closed circles), or ZnMP-5gly-Bfr dimer (open symbols) at the indicated concentrations. All solutions contained 0.1 M TEOA, and 2 mM MV in 50 mM MES pH 6, 0.5 M NaCl. Solutions were continuously irradiated with a 300 W

halogen lamp (3.8 mW/cm^2) at room temperature. Data points are the average from six experiments with standard deviations indicated by vertical bars.

Based on these "one-pot" results, we reasoned that the H$_2$ production proceeded as diagrammed in Scheme 4, in which reduction of MV^{2+} by TEOA was photoinduced via the ZnMP-5gly-Bfr dimer, and H$_2$ generation occurred in a subsequent "dark" reaction at Pt NP@5gly-Bfr 24-mer using MV$^+$ as the electron donor. Since the "dark" reaction at the Pt NPs presumably does not require ZnP, we also reasoned that separately prepared porphyrin-free PtNP@wtBfr 24-mer (characterized as shown in Figure 3B, Figure 5B, and Figure S4B) should be functional in photosensitized H$_2$ generation when mixed with ZnMP-5gly-Bfr dimer. Indeed, continuous visible light irradiation of this "two-pot" mixture in the presence of MV and TEOA under anaerobic conditions resulted in robust photosensitized production of H$_2$ (Figure 6, "two-pot" panel). 7 hours irradiation with 10 μM of 5gly-ZnP-Bfr dimer mixed with porphyrin-free Pt NP@wtBfr 24-mer at 20 μM Pt generated ~1 micromol H$_2$. This yield represents a turnover of ~33 H$_2$/ZnMP. Doubling the concentration of ZnMP to 20 μM approximately doubled the amount of photo-induced H$_2$ produced after 7 hours. Loss of the porphyrin Soret absorption was significantly slower in the "two-pot" system compared to the "one-pot" system, and the Soret band was still prominent after 7 hours irradiation. Similar "two-pot" H$_2$ production was obtained using ZnPP-5gly-Bfr dimer in place of ZnMP-5gly-Bfr dimer (Figure S7). As was the case for the "one-pot" system, no H$_2$ was detected in "two-pot" mixtures using as-isolated ZnP-Bfr dimer in place of ZnP-5gly-Bfr dimer during 4 hours of irradiation.

Scheme 4

ZnP-5gly-
Bfr dimer

Pt NP@Bfr
24-mer
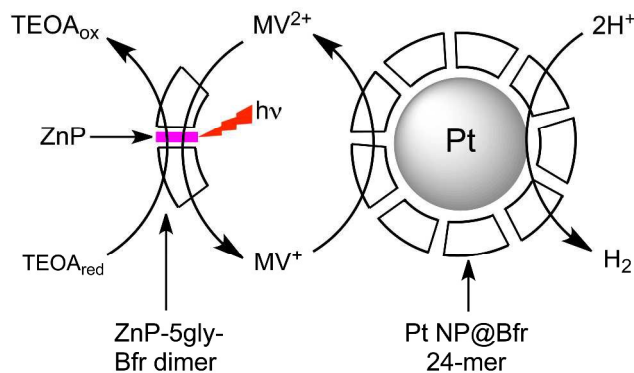
Conclusions

Our "two-pot" results thus support the photosensitized H_2 generation pathway shown in Scheme 4 that we surmised for the "one-pot" system. Photosensitization occurred via a ZnP-Bfr dimer modified to increase the exposure of the porphyrin vinyl side. This modification apparently increased the efficiency of photo-induced electron transfer events. "Two-pot" mixtures containing separately prepared Pt-free ZnP-5gly-Bfr dimer and porphyrin-free Pt NP@wtBfr 24-mer exhibited higher H_2 yields and turnover frequencies per Pt, as well as more sustained H_2 generation than the optimized "one-pot" mixtures. However both systems exhibited turnover frequencies comparable to those of other systems operating according to Scheme 1 using protein-bound porphyrins combined with synthetic polymer-coated Pt NPs.[12, 13, 15] In fact, we obtained yields of H_2 comparable to those in our "two-pot" system when we substituted poly(vinyl)alcohol-coated Pt NPs[40] in place of porphyrin-free Pt NP@wtBfr at approximately the same Pt concentration (data not shown). "Dark" electron transfer from external MV^+ across the wtBfr protein shell to the internalized Pt NPs is, therefore, apparently sufficient to support H_2 generation according to Scheme 4. Our results demonstrate a unique protein-based photosensitizer/Pt NP system that is easily assembled and readily modifiable for photosensitized

redox chemistry. We are in the process of exploring additional amino acid substitutions and other modification to the ZnP environment and to the Bfr proteins shell that could improve and expand the photochemical performance of this novel system.

References

1.   D. G. Nocera, *Acc. Chem. Res.*, 2012, **45**, 767-776.

2.   K. Bren, *Interface Focus*, 2015, DOI: 10.1098/rsfs.2014.0091, 20140091.

3.   A. Onoda and T. Hayashi, *Curr. Opin. Chem. Biol.*, 2015, **25**, 133-140.

4.   L. M. Utschig, S. R. Soltau and D. M. Tiede, *Curr. Opin. Chem. Biol.*, 2015, **25**, 1-8.

5.   S. Fukuzumi, *Curr. Opin. Chem. Biol.*, 2015, **25**, 18-26.

6.   M. Gorka, J. Schartner, A. van der Est, M. Rogner and J. H. Golbeck, *Biochemistry*, 2014, **53**, 2295-2306.

7.   P. A. Angaridis, T. Lazarides and A. C. Coutsolelos, *Polyhedron*, 2014, **82**, 19-32.

8.   K. Ladomenou, M. Natali, E. Iengo, G. Charalampidis, F. Scandola and A. G. Coutsolelos, *Coord. Chem. Rev.*, 2015, DOI: 10.1016/j.ccr.2014.10.001, in press.

9.   K. Kalyanasundaram and M. Grätzel, *Helv. Chim. Acta*, 1980, **63**, 478-485.

10.   G. Mclendon and D. S. Miller, *J. Chem. Soc. Chem. Comm.*, 1980, 533-534.

11.   J. R. Darwent, P. Douglas, A. Harriman, G. Porter and M. C. Richoux, *Coord. Chem. Rev.*, 1982, **44**, 83-126.

12.   T. Komatsu, R. M. Wang, P. A. Zunszain, S. Curry and E. Tsuchida, *J. Am. Chem. Soc.*, 2006, **128**, 16297-16301.

13.   T. Matsuo, A. Asano, T. Ando, Y. Hisaeda and T. Hayashi, *Chem. Commun.*, 2008, 3684-3686.

14.   D. S. Miller and G. Mclendon, *J. Am. Chem. Soc.*, 1981, **103**, 6791-6796.

15.   H. Yamaguchi, T. Onji, H. Ohara, N. Ikeda and A. Harada, *Bull. Chem. Soc. Jap.*, 2009, **82**, 1341-1346.

16.   L. B. Zhang, L. Laug, W. Munchgesang, E. Pippel, U. Gosele, M. Brandsch and M. Knez, *Nano Lett.*, 2010, **10**, 219-223.

17.   Z. Yang, X. Y. Wang, H. J. Diao, J. F. Zhang, H. Y. Li, H. Z. Sun and Z. J. Guo, *Chem. Commun.*, 2007, 3453-3455.

18.   Q. Y. Deng, B. Yang, J. F. Wang, C. G. Whiteley and X. N. Wang, *Biotechnol. Lett.*, 2009, **31**, 1505-1509.

19.   Z. Varpness, J. W. Peters, M. Young and T. Douglas, *Nano Lett.*, 2005, **5**, 2306-2309.

20.   M. Young, S. Kang, J. Lucon, Z. B. Varpness, L. Liepold, M. Uchida, D. Willits and T. Douglas, *Angew. Chem. Int. Ed. Eng.*, 2008, **47**, 7845-7848.

21.   Z. Varpness, C. Shoopman, J. W. Peters, M. Young and T. Douglas, in *Biomolecular Catalysis: Nanoscale Science and Technology*, eds. J. Kim, S. H. Kim and P. Wang, American Chemical Society, Washington, DC, 2008, vol. 982, ch. 17, pp. 263-272.

22.   K. H. Ebrahimi, P. L. Hagedoorn and W. R. Hagen, *Chem. Rev.*, 2015, **115**, 295-326.

23.   S. Baaghil, A. Lewin, G. R. Moore and N. E. Le Brun, *Biochemistry*, 2003, **42**, 14047-14056.

24.   J. M. Bradley, G. R. Moore and N. E. Le Brun, *J. Biol Inorg. Chem.*, 2014, **19**, 775-785.

25.   S. C. Andrews, N. E. Le Brun, V. Barynin, A. J. Thomson, G. R. Moore, J. R. Guest and P. M. Harrison, *J. Biol. Chem.*, 1995, **270**, 23268-23274.

26.   S. G. Wong, S. A. Tom-Yew, A. Lewin, N. E. Le Brun, G. R. Moore, M. E. Murphy and A. G. Mauk, *J. Biol. Chem.*, 2009, **284**, 18873-18881.

27.   S. C. Willies, M. N. Isupov, E. F. Garman and J. A. Littlechild, *J. Biol Inorg. Chem.*, 2009, **14**, 201-207.

28.   F. Frolow, A. J. Kalb and J. Yariv, *Nature Struct. Biol.*, 1994, **1**, 453-460.

29.   A. Dautant, J. B. Meyer, J. Yariv, G. Precigoux, R. M. Sweet, A. J. Kalb and F. Frolow, *Acta Crystallogr. D*, 1998, **54**, 16-24.

30.   B. Conlan, N. Cox, J. H. Su, W. Hillier, J. Messinger, W. Lubitz, P. L. Dutton and T. Wydrzynski, *Biochim. Biophys. Acta*, 2009, **1787**, 1112-1121.

31.   J. J. Leonard, T. Yonetani and J. B. Callis, *Biochemistry*, 1974, **13**, 1460-1464.

32.   R. P. Garg, C. J. Vargo, X. Y. Cui and D. M. Kurtz, Jr., *Biochemistry*, 1996, **35**, 6297-6301.

33.   S. Tabor, in *Current Protocols in Molecular Biology*, eds. F. A. Ausubel, R. Brent, R. E. Kingston, D. D. Moore, J. G. Seidman, J. A. Smith and K. Struhl, Green Publishing and Wiley-Interscience, New York, 1990, ch. 16, pp. 16.12.11-16.12.11.

34.   E. A. Berry and B. L. Trumpower, *Anal. Biochem.*, 1987, **161**, 1-15.

35.   L. L. Stookey, *Anal. Chem.*, 1970, **42**, 779-781.

36.   H. Anni, J. M. Vanderkooi and L. Mayne, *Biochemistry*, 1995, **34**, 5744-5753.

37.   J. M. Nocek, B. P. Sishta, J. C. Cameron, A. G. Mauk and B. M. Hoffmann, *J. Am. Chem. Soc.*, 1997, **119**, 2146-2155.

38.   E. A. Della Pia, Q. J. Chi, M. Elliott, J. E. Macdonald, J. Ulstrup and D. D. Jones, *Chem. Commun.*, 2012, **48**, 10624-10626.

39.   R. E. Sharp, J. R. Diers, D. F. Bocian and P. L. Dutton, *J. Am. Chem. Soc.*, 1998, **120**, 7103-7104.

40.   Y. L. Luo and X. P. Sun, *Mater. Lett.*, 2007, **61**, 2015-2017.

Graphical Abstract

Photosensitized H_2 generation can be sustained for several hours in aqueous solution using a protein scaffold that nucleates formation of platinum nanoparticles (Pt NPs) and contains "built-in" zinc-porphyrin photosensitizers.